ISSN 1674-1056
http://cpb.iphy.ac.cn
http://iopscience.iop.org/cpb
中国物理 B
Chinese Physics
中国物理
Chinese Physics B

Propagation characteristics of oblique incidence terahertz wave through non-uniform plasma

Antao Chen(陈安涛), Haoyu Sun(孙浩宇), Yiping Han(韩一平), Jiajie Wang(汪加洁), Zhiwei Cui(崔志伟)

Citation: Chin. Phys. B . 2019, 28(1): 014201. **doi:** 10.1088/1674-1056/28/1/014201
Journal homepage: http://cpb.iphy.ac.cn; http://iopscience.iop.org/cpb

What follows is a list of articles you may be interested in

Rapid measurement of transmission matrix with the sequential semi-definite programming method

Zhenfeng Zhang(张振峰), Bin Zhang(张彬), Qi Feng(冯祺), Huimei He(何惠梅), Yingchun Ding(丁迎春)\
Chin. Phys. B . 2018, 27(8): 084201. **doi:** 10.1088/1674-1056/27/8/084201

Coupled resonator-induced transparency on a three-ring resonator

Xinquan Jiao(焦新泉), Haobo Yu(于皓博), Miao Yu(于淼), Chenyang Xue(薛晨阳), Yongfeng Ren(任勇峰)
Chin. Phys. B . 2018, 27(7): 074212. **doi:** 10.1088/1674-1056/27/7/074212

Influence of intra-cavity loss on transmission characteristics of fiber Bragg grating Fabry-Perot cavity

Di Wang(王迪), Meng Ding(丁孟), Hao-Yang Pi(皮浩洋), Xuan Li(李璇), Fei Yang(杨飞), Qing Ye(叶青), Hai-Wen Cai(蔡海文), Fang Wei(魏芳)
Chin. Phys. B . 2018, 27(2): 024207. **doi:** 10.1088/1674-1056/27/2/024207

Optical properties of a three-dimensional chiral metamaterial

Juan-Juan Guo(郭娟娟), Mao-Sheng Wang(汪茂胜), Wan-Xia Huang(黄万霞)
Chin. Phys. B . 2017, 26(12): 124211. **doi:** 10.1088/1674-1056/26/12/124211

Low-loss terahertz waveguide with InAs-graphene-SiC structure

Xu De-Gang, Wang Yu-Ye, Yu Hong, Li Jia-Qi, Li Zhong-Xiao, Yan Chao, Zhang Hao, Liu Peng-Xiang, Zhong Kai, Wang Wei-Peng, Yao Jian-Quan
Chin. Phys. B . 2014, 23(5): 054210. **doi:** 10.1088/1674-1056/23/5/054210

Propagation characteristics of oblique incidence terahertz wave through non-uniform plasma*

Antao Chen(陈安涛), Haoyu Sun(孙浩宇), Yiping Han(韩一平)†,
Jiajie Wang(汪加洁)‡, and Zhiwei Cui(崔志伟)

School of Physics and Optoelectronic Engineering, Xidian University, Xi'an 710071, *China*

(Received 3 September 2018; revised manuscript received 28 October 2018; published online 12 December 2018)

The propagation characteristics of oblique incidence terahertz (THz) waves through non-uniform plasma are investigated by the shift-operator finite-difference time-domain (SO-FDTD) method combined with the phase matching condition. The electron density distribution of the non-uniform plasma is assumed to be in a Gaussian profile. Validation of the present method is performed by comparing the results with those obtained by an analytical method for a homogeneous plasma slab. Then the effects of parameters of THz wave and plasma layer on the propagation properties are analyzed. It is found that the transmission coefficients greatly depend on the incident angle as well as on the thickness of the plasma, while the polarization of the incident wave has little influence on the propagation process in the range of frequency considered in this paper. The results confirm that the THz wave can pass through the plasma sheath effectively under certain conditions, which makes it a potential candidate to overcome the ionization blackout problem.

Keywords: terahertz wave, transmission, oblique incidence, plasma sheath, finite-difference time-domain method

PACS: 42.25.Bs, 03.50.De, 02.70.Bf **DOI:** 10.1088/1674-1056/28/1/014201

1. Introduction

When vehicles fly at hypersonic velocities within the atmosphere, they become enveloped in a plasma sheath that prevents radio communication between the aerospace and the ground control center, which is the well-known blackout problem.[1–4] In order to mitigate or eliminate the reentry blackout problem, a number of techniques have been proposed, such as high power, high frequencies, low frequencies, lasers, magnetic fields, and so on.[3,5–7] The terahertz wave (THz), commonly referred to as T-rays, sub-millimeter, or far infrared, refers to the electromagnetic radiation at the frequency from 0.1 THz to 10 THz, has attracted much attention recently partially because it is one of the potential candidates in the high frequencies communication methods. The techniques for the generation of THz wave were developed rapidly in recent years[8–11] and promising applications of THz waves can be found in various fields.[12] As the basis of communication between the hypersonic vehicles and the ground control center, the interaction between plasma and THz wave (absorption, reflection, and transmission) is a key issue to be analyzed. Over the past few years, the propagation characteristics of the THz wave in plasma have been investigated by different methodologies, such as the analytical method,[13–17] experimental method,[18] scattering matrix method (SMM),[19,20] propagation matrix method (PMM),[21] finite-difference time-domain (FDTD) method,[22–28] Wentzel–Kramer–Brillouin (WKB) method,[29,30] and so on.

The FDTD method has been widely used to solve the interaction problems between the THz wave and plasma because of its capability in simulating the propagation characteristics of a wideband THz wave through inhomogeneous dispersive plasma. Wang *et al.*[22,27,28] investigated the propagation properties of the THz wave in a time-varying dusty plasma slab using the auxiliary differential equation finite-difference time-domain (ADE-FDTD) method. Zheng *et al.*[23] studied the propagation characteristics of the THz wave in unmagnetized plasma by the Z transform finite-difference time-domain (ZT-FDTD) method. Theoretical results were compared with experimental measurements in Ref. [20], where good agreements were achieved. The broadband propagation characteristics of the THz wave in an anisotropic magnetized plasma were investigated by Tian *et al.*[24] using the JE convolution FDTD (JEC-FDTD) method. Gao *et al.*[25] investigated the characteristics of reflection, transmission, and absorption of THz waves in a sandwich type microplasma structure by the ZT-FDTD method.

Although studies of propagation characteristics of the THz wave in plasma media can be found in several works, most of the previous research focused on the normally incident wave cases, i.e., the incident plane wave propagates at an angle of zero with respect to the normal of the media interfaces, lim-

*Project supported by the National Basic Research Program of China (Grant No. 2014CB340203), the National Natural Science Foundation of China (Grant Nos. 61431010 and 61501350), and the Natural Science Foundation of Shaanxi Province, China (Grant Nos. 2018JM6016 and 2016JM1001).

†Corresponding author. E-mail: yphan@xidian.edu.cn

‡Corresponding author. E-mail: wangjiajie@xidian.edu.cn

© 2019 Chinese Physical Society and IOP Publishing Ltd

ited attention was paid to the oblique incidence cases. In practice, the angle of incidence changes over a wide range during flight, which indicates that the oblique incidence wave cases require more consideration. Recently, using the impedance matching method, Rahmani *et al.*[31] investigated the transmission, reflection, and absorption of s-polarized wave obliquely incident on the plasma slab which has a bell-like electron density distribution. The SMM was adopted by Yuan *et al.*[32] to analyze the transmission of obliquely incident THz waves in the plasma sheaths covering a blunt coned vehicle, in which the plasma sheaths were generated based on a hypersonic fluid model. Cao *et al.*[33] studied the propagation characteristics of obliquely incident THz waves though dusty plasma using the PMM, where the electron density distribution of the dusty plasma was assumed to be parabolic. Based on the twice reflection model, Tian *et al.*[34] investigated the obliquely incident wave through a nonuniform magnetized plasma slab, in which both the electron density and the collision frequency across the plasma were assumed to be in a Gaussian profile. To solve the problem under study, the non-uniform plasma was divided into a series of layers with uniform electron density.[34] Nevertheless, this dividing method fails when one encounters plasma with a high gradient electron density distribution. To overcome this difficulty, the FDTD is a good choice.

The THz wave obliquely incident on a plasma sheath, which is non-uniform in half space, is a two-dimensional problem for the FDTD method. Thus it will cost a lot of memory and computation time in the simulation. To save computational memory and time, in this paper, the FDTD method combined with the phase matching condition is utilized to solve the propagation problem of obliquely incident THz waves through an inhomogeneous plasma. With the help of phase matching condition, the problem is simplified to a pseudo one-dimensional problem, which can greatly reduce the memory required and improve the efficiency. To describe the distribution of the electron density in an inhomogeneous plasma, the Gaussian profile is introduced which corresponds to the flow field around the hypersonic aircraft at a high altitude of space.[35]

The rest of this paper is structured as follows. In Section 2, the physical model of the propagation problem is given, with a brief description of the method used in solving the problem under study. Numerical results and discussions concerning the transmission features of the THz wave through an inhomogeneous plasma are presented in Section 3. Section 4 concludes this paper.

2. Physical model and methods

A geometric sketch of the problem under study is shown in Fig. 1, where a plane THz wave propagates through a plasma sheath around the hypersonic vehicle at an arbitrary incident angle. The plasma sheath is non-uniform in half space, which is inhomogeneous in y direction and uniform in x and z directions. The thickness of the plasma sheath is d in y direction and infinite in the other two directions. The incident THz wave is assumed to propagate through the plasma sheath in the plane of xoy at an incident angle θ with respect to the normal of the plasma sheath interfaces.

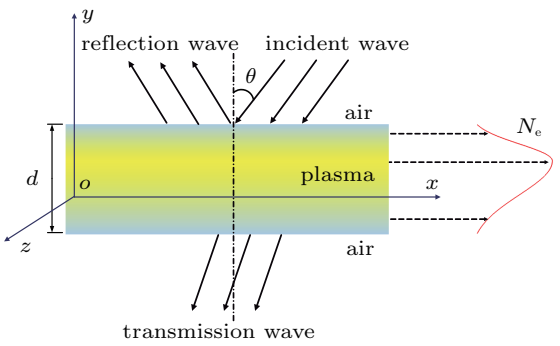


Fig. 1. Schematic diagram of a THz wave propagating through nonuniform plasma layer.

As shown in Fig. 1, when the THz wave propagates through the plasma slab in the xoy plane, the electric field $\boldsymbol{E}$ and magnetic field $\boldsymbol{H}$ satisfy $\partial \boldsymbol{E}/\partial z = 0$ and $\partial \boldsymbol{H}/\partial z = 0$, in which $\partial/\partial z$ means derivative to z. The fields in the plasma sheath can be divided to two modes: (i) the transverse magnetic (TM_z) mode, which is composed of E_z, H_x, H_y, and (ii) the transverse electric (TE_z) mode, which is composed of H_z, E_x, E_y. In the following, we will only consider the TE_z mode case since the TM_z case can be obtained in the same manner.

The fields in plasma can be described by Maxwell's equations in the frequency domain

$$\frac{\partial H_z}{\partial y} = \mathrm{j}\omega D_x = \mathrm{j}\omega\varepsilon_0\varepsilon_\mathrm{r}(y,\omega)E_x, \tag{1}$$

$$\frac{\partial H_z}{\partial x} = -\mathrm{j}\omega\varepsilon_0\varepsilon_\mathrm{r}(y,\omega)E_y, \tag{2}$$

$$\frac{\partial E_y}{\partial x} - \frac{\partial E_x}{\partial y} = -\mathrm{j}\omega\mu_0\mu_\mathrm{r}H_z, \tag{3}$$

where $\boldsymbol{D}$ is the electric flux density, ε_0 is the vacuum permittivity, ε_r is the relative permittivity of the medium, μ_0 is the magnetic permeability of vacuum, and ω is the angular frequency of the incident wave. For the medium considered in this paper, i.e., nonmagnetic plasma, the relative magnetic permeability is $\mu_\mathrm{r} = 1$.

For the TE_z mode, the propagation equation in the xoy plane can be expressed as

$$H_z = H_0 \exp[\mathrm{j}(\omega t - \boldsymbol{k}\cdot\boldsymbol{r})], \tag{4}$$

where H_0 is the amplitude of the magnetic field, $\boldsymbol{k}$ is the wave number in plasma, and $\boldsymbol{r} = x\cdot\boldsymbol{x} + y\cdot\boldsymbol{y}$. The time factor

$\exp(\mathrm{j}\omega t)$ is omitted and the magnetic field component of the incident plane wave in plasma is expressed as

$$H_z = H_0 \exp(\mathrm{j}k_x x + \mathrm{j}k_y y) \cdot \exp(\mathrm{j}\omega t). \tag{5}$$

Based on the transformations $\partial/\partial x \to \mathrm{j}k_x$ and $\partial/\partial t \to \mathrm{j}\omega$, the derivative of Eq. (2) to x in plasma is

$$\mathrm{j}\omega\varepsilon_0\varepsilon_\mathrm{r}\frac{\partial E_y}{\partial x} = k_x^2 H_z. \tag{6}$$

Based on the phase matching condition, the phase velocity in the direction parallel to the media interfaces is constant that $k_x = k_\mathrm{air}\sin\theta$. Substituting Eq. (6) into Eq. (3) yields

$$\mathrm{j}\omega\mu_0\left(\mu_\mathrm{r} - \frac{\sin^2\theta}{\varepsilon_\mathrm{r}(\omega)}\right)H_z = \frac{\partial E_x}{\partial y}. \tag{7}$$

For simplicity, two new auxiliary variables $\tilde{B}$ and $\tilde{\mu}_\mathrm{r}$ are defined as

$$\tilde{B}_z(\omega) = \mu_0\tilde{\mu}_\mathrm{r}(\omega)H_z(\omega), \tag{8}$$

$$\tilde{\mu}_\mathrm{r}(\omega) = \mu_\mathrm{r} - \frac{\sin^2\theta}{\varepsilon_\mathrm{r}(\omega)}. \tag{9}$$

Substituting Eqs. (8) and (9) into Eq. (7) yields

$$\mathrm{j}\omega\tilde{B}_z = \frac{\partial E_x}{\partial y}. \tag{10}$$

Equations (1) and (10) are then transformed into time domain and written as

$$\frac{\partial H_z(x,y,t)}{\partial y} = \varepsilon_0\frac{\partial[\varepsilon_\mathrm{r}(y,t) * E_x(x,y,t)]}{\partial t} = \frac{\partial D_x(x,y,t)}{\partial t}, \tag{11}$$

$$\frac{\partial\tilde{B}_z(x,y,t)}{\partial t} = \frac{\partial E_x(x,y,t)}{\partial y}, \tag{12}$$

where $*$ represents convolution.

The permittivity of unmagnetized plasma is given as[36]

$$\begin{aligned}\varepsilon_{\mathrm{r,p}}(\omega) &= \varepsilon_0\left(\varepsilon_\infty + \frac{\omega_\mathrm{p}^2}{\omega(\mathrm{j}\upsilon_\mathrm{c} - \omega)}\right)\\ &= \frac{\omega_\mathrm{p}^2 + \varepsilon_\infty\upsilon_\mathrm{c}(\mathrm{j}\omega) + \varepsilon_\infty(\mathrm{j}\omega)^2}{\upsilon_\mathrm{c}(\mathrm{j}\omega) + (\mathrm{j}\omega)^2},\end{aligned} \tag{13}$$

where ε_∞ is the infinite-frequency limit of the relative permittivity; $\omega_\mathrm{p} = 2\pi f_\mathrm{p}$, f_p is the plasma frequency, and υ_c is the electron collision frequency.

Substituting Eq. (13) into Eq. (9) yields

$$\begin{aligned}\tilde{\mu}_{\mathrm{r,p}}(\omega) &= 1 - \frac{\sin^2\theta}{\dfrac{\omega_\mathrm{p}^2 + \varepsilon_\infty\upsilon_\mathrm{c}(\mathrm{j}\omega) + \varepsilon_\infty(\mathrm{j}\omega)^2}{\upsilon_\mathrm{c}(\mathrm{j}\omega) + (\mathrm{j}\omega)^2}}\\ &= \frac{\omega_\mathrm{p}^2 + (\varepsilon_\infty\upsilon_\mathrm{c} - \sin^2\theta\,\upsilon_\mathrm{c})(\mathrm{j}\omega) + (\varepsilon_\infty - \sin^2\theta)(\mathrm{j}\omega)^2}{\omega_\mathrm{p}^2 + \varepsilon_\infty\upsilon_\mathrm{c}(\mathrm{j}\omega) + \varepsilon_\infty(\mathrm{j}\omega)^2}.\end{aligned} \tag{14}$$

The electric flux density D_x and the auxiliary variable $\tilde{B}_\mathrm{z}$ can be written as

$$D_x(\omega) = \varepsilon_0\varepsilon_{\mathrm{r,p}}(\omega)E_x(\omega) = \varepsilon_0\frac{\sum_{n=0}^{N} p_n^E(\mathrm{j}\omega)^n}{\sum_{m=0}^{M} q_m^E(\mathrm{j}\omega)^m}E_x(\omega), \tag{15}$$

$$\tilde{B}_z(\omega) = \mu_0\tilde{\mu}_{\mathrm{r,p}}(\omega)H_z(\omega) = \mu_0\frac{\sum_{n=0}^{N} p_n^H(\mathrm{j}\omega)^n}{\sum_{m=0}^{M} q_m^H(\mathrm{j}\omega)^m}H_z(\omega). \tag{16}$$

Comparing Eqs. (13) and (14) with Eqs. (15) and (16), we can obtain that $M = N = 2$ and

$$\begin{aligned}&p_0^E = \omega_\mathrm{p}^2, && p_0^H = \omega_\mathrm{p}^2,\\ &p_1^E = \varepsilon_\infty\upsilon_\mathrm{c}, && p_1^H = \varepsilon_\infty\upsilon_\mathrm{c} - \sin^2\theta\,\upsilon_\mathrm{c},\\ &p_2^E = \varepsilon_\infty, && p_2^H = \varepsilon_\infty - \sin^2\theta,\\ &q_0^E = 0, && q_0^H = \omega_\mathrm{p}^2,\\ &q_1^E = \upsilon_\mathrm{c}, && q_1^H = \varepsilon_\infty\upsilon_\mathrm{c},\\ &q_2^E = 1, && q_2^H = \varepsilon_\infty.\end{aligned} \tag{17}$$

With the transition relationship from the frequency domain to time domain, $\mathrm{j}\omega \to \partial/\partial t$, we can obtain the expressive forms of Eqs. (15) and (16) in the time domain

$$D_x(t) = \varepsilon_0\varepsilon_{\mathrm{r,p}}\frac{\partial}{\partial t}E_x(t) = \varepsilon_0\frac{\sum_{n=0}^{N} p_n^E\left(\frac{\partial}{\partial t}\right)^n}{\sum_{m=0}^{M} q_m^E\left(\frac{\partial}{\partial t}\right)^m}E_x(t), \tag{18}$$

$$\tilde{B}_z(t) = \mu_0\tilde{\mu}_{\mathrm{r,p}}\frac{\partial}{\partial t}H_z(t) = \mu_0\frac{\sum_{n=0}^{N} p_n^H\left(\frac{\partial}{\partial t}\right)^n}{\sum_{m=0}^{M} q_m^H\left(\frac{\partial}{\partial t}\right)^m}H_z(t). \tag{19}$$

If we assume that the function in the time domain has the form

$$y(t) = \frac{\partial f(t)}{\partial t}. \tag{20}$$

The central difference of Eq. (20) at $(n+1/2)\Delta t$ can be approximately expressed as

$$\frac{y^{n+1} + y^n}{2} = \frac{f^{n+1} - f^n}{\Delta t}. \tag{21}$$

Now, we introduce the shift arithmetic operators z_t,

$$z_t f^n = f^{n+1}. \tag{22}$$

Combining Eqs. (21) and (22), we can obtain

$$y^n = \left(\frac{2}{\Delta t}\frac{z_t - 1}{z_t + 1}\right)f^n. \tag{23}$$

Comparing Eq. (23) with Eq. (20), we can have

$$\frac{\partial}{\partial t} \to \frac{2}{\Delta t}\frac{z_t - 1}{z_t + 1}. \tag{24}$$

By substituting (24) into Eqs. (18) and (19), and multiplying $(z_t+1)^N$ on either side of the equal sign, we can obtain the constitutive relationship of dispersion in the time domain as

$$\left[\sum_{l=0}^{M} q_l \left(h\frac{z_t-1}{z_t+1}\right)^l\right] D_x^n = \varepsilon_0 \left[\sum_{l=0}^{N} p_l \left(h\frac{z_t-1}{z_t+1}\right)^l\right] E_x^n, \tag{25}$$

$$\left[\sum_{l=0}^{M} q_l h^l (z_t+1)^{N-l}(z_t-1)^l\right] D_x^n = \varepsilon_0 \left[\sum_{l=0}^{N} p_l h^l (z_t+1)^{N-l}(z_t-1)^l\right] E_x^n. \tag{26}$$

Based on the relationship

$$z_t^k D_x^n \to z_t^{k-1} D_x^{n+1} \to D_x^{n+k}, \tag{27}$$

the solution of E_x^{n+1} can be obtained as

$$E_x^{n+1} = \frac{1}{b_0^E}\left[\sum_{l=0}^{M} \frac{a_l^E}{\varepsilon_0} D_x^{n+1-l} - \sum_{l=1}^{N} b_l^E E_x^{n+1-l}\right]. \tag{28}$$

The expression of H_x^{n+1} can be obtained in the same way as

$$H_{x,z}^{n+1} = \frac{1}{b_0^H}\left[\sum_{l=0}^{M} \frac{a_l^H}{\mu_0} \tilde{B}_{x,z}^{n+1-l} - \sum_{l=1}^{N} b_l^H H_{x,z}^{n+1-l}\right], \tag{29}$$

where

$$\begin{aligned} a_0^{E,H} &= q_0^{E,H} + q_1^{E,H} h + q_2^{E,H} h^2, \\ a_1^{E,H} &= 2q_0^{E,H} - 2q_2^{E,H} h^2, \\ a_2^{E,H} &= q_0^{E,H} - q_1^{E,H} h + q_2^{E,H} h^2, \\ b_0^{E,H} &= p_0^{E,H} + p_1^{E,H} h + p_2^{E,H} h^2, \\ b_1^{E,H} &= 2p_0^{E,H} - 2p_2^{E,H} h^2, \\ b_2^{E,H} &= p_0^{E,H} - p_1^{E,H} h + p_2^{E,H} h^2. \end{aligned} \tag{30}$$

For the TE case, the incident magnetic field $H_{z,\mathrm{i}}$, reflected magnetic field $H_{z,\mathrm{r}}$, and transmitted magnetic field $H_{z,\mathrm{t}}$ are recorded during the time iteration. By using the Fourier transform, the transmission coefficient T and reflection coefficient R can be obtained by

$$T(f) = H_{z,\mathrm{t}}(f)/H_{z,\mathrm{i}}(f), \tag{31}$$

$$R(f) = H_{z,\mathrm{r}}(f)/H_{z,\mathrm{i}}(f), \tag{32}$$

where f is the frequency of the THz wave. Then the absorption coefficient is calculated by

$$A(f) = 1 - T(f) - R(f). \tag{33}$$

For the TM case, the transmission coefficient and absorption coefficient can be calculated in the same way by substituting electric field E_z for magnetic field H_z.

3. Numerical results and discussion

Numerical simulations are implemented based on the theoretical treatments presented in Section 2. The incident THz wave of cosine-modulated Gaussian pulse in the SO-FDTD is given by

$$E(t) = \cos(2\pi f_{\mathrm{mid}} t)\cdot \exp\left[-\frac{(t-t_0)^2}{\tau^2}\right], \tag{34}$$

where $f_{\mathrm{mid}} = 5.5\times 10^{11}$Hz is the central frequency of the pulse, $\tau = 0.966/\Delta f$ stands for the width of the pulse, and $t_0 = 4.5\tau$ is the time of the peak. Here Δf is the width of the frequency needed in the simulations and $\Delta f = 9\times 10^{11}$ Hz. In what follows, this cosine-modulated Gaussian pulse incident wave is used in all the simulations.

3.1. Validity of the proposed method

Before we start to analyze the propagation characteristics of the THz wave through an inhomogeneous plasma, the validity of the method adopted in this paper is verified by comparing the results obtained by our method with those obtained by an analytical method.[35] The propagation characteristics of THz waves with different incident angles in a homogeneous plasma slab are taken into consideration.

The FDTD problem space consists of 474 cells, and the homogeneous plasma occupies 71–404 cells. The cell size is $\Delta y = 1.5\times 10^{-5}$ m, and the thickness of the plasma layer is 5 mm. Both ends of the cell space are treated by uniaxial perfectly matched layer absorbing boundary condition to eliminate unwanted reflections. The plasma parameters are

$$\begin{aligned} N_{\mathrm{e}} &= 0.18\times 10^{21}\ \mathrm{m}^{-3}, \\ \upsilon_{\mathrm{c}} &= 5\times 10^{11}\ \mathrm{Hz}. \end{aligned} \tag{35}$$

Comparisons of the transmission coefficients of the THz wave in the plasma slab calculated by our method and those obtained using the analytical solution are displayed in Fig. 2. As shown in Fig. 2, very good agreements are achieved for both TE and TM waves, which partially indicates the correctness of our method.

The plasma density stemmed from the reentry hypersonic flight in the stagnation region could reach 10^{21} m^{-3} and the plasma frequency corresponding to this electron density can reach 0.28 THz.[24] In the following simulations, the Gaussian electron density profile is chosen to stand for the variation of electron density, which corresponds to the non-uniform plasma flow field around the hypersonic aircraft at a high altitude of space[35]

$$n_{\mathrm{e}}(y) = \begin{cases} n_{\mathrm{emax}}\,\mathrm{e}^{-\alpha_1^2 y^2}, & y_1 \leqslant y \leqslant 0, \\ n_{\mathrm{emax}}\,\mathrm{e}^{-\alpha_2^2 y^2}, & 0 \leqslant y \leqslant y_2, \end{cases} \tag{36}$$

where $d = y_2 - y_1 = 8$ cm is the thickness of the plasma, $y_1 = -d/5$, $y_2 = 4d/5$, $\alpha_1 = \sqrt{2.3}/y_1$, $\alpha_2 = \sqrt{2.3}/y_2$, in which α_1

and α_2 represent the distribution form of electron density. The maximum electron density is assumed to be $n_{\mathrm{emax}} = 10^{21}$ m^{-3}. The distribution of Gaussian profile is plotted in Fig. 3, in which the collision frequency is $\upsilon_{\mathrm{c}} = 1.5 \times 10^{10}$ Hz, and the plasma frequency ω_{p} is calculated as

$$\omega_{\mathrm{p}} = 56.3808 \times \sqrt{n_{\mathrm{e}}} \quad (\mathrm{rad/s}). \tag{37}$$

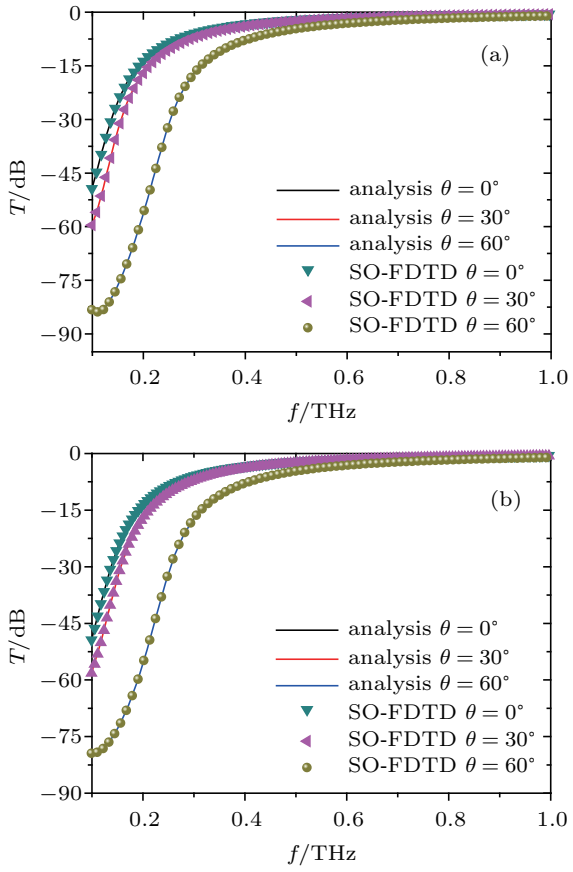


Fig. 2. Comparisons of the transmission coefficients of a plasma slab versus the incident angles between analytical solutions and SO-FDTD method: (a) TE wave, (b) TM wave.

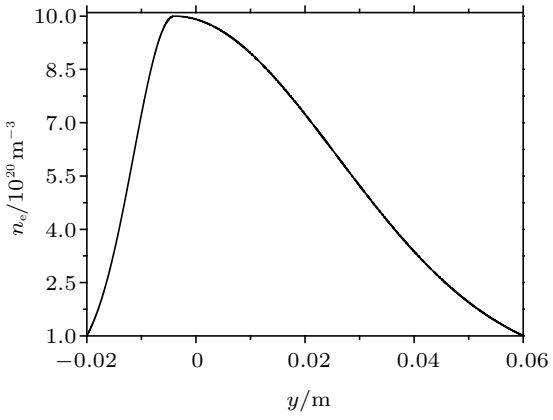


Fig. 3. Plasma electron density distribution in Gaussian profile.

3.2. Influences of incident angle

In order to investigate the influence of the incident angle on the propagation characteristics of a THz wave in plasma, the incident angle of the THz wave is varied in steps of 15° from 0° to 90° in the simulations. The transmission and absorption coefficients for TE wave are calculated and shown in Fig. 4 for $\theta = 0°$, 15°, 30°, and 45°. As shown in Fig. 4(a), the transmission coefficient increases as the incident angle decreases or the frequency of the THz wave increases. When the incident wave frequency approaches 1 THz, the transmission coefficient tends to 0 dB, which indicates that the THz wave can be used to release the blackout problem. For the normal incidence case, when the frequency of the incident wave is $f = 0.3$ THz, the transmission coefficient $T \approx -20$ dB. As the incident wave frequency increases, the transmission coefficient increases and tends to 0 dB. However, for $\theta > 15°$ cases, when $f = 0.3$ THz, the transmission coefficient is far less than -20 dB, which indicates that the THz wave cannot penetrate the plasma. As shown in Fig. 4(b), the absorption coefficient increases at first and then decreases as the incident frequency increases. For each incident angle case, there is a maximum absorption coefficient, and the corresponding frequency moves to a larger value as the incident angle increases. It indicates that when a THz wave is used in communication through plasma, the frequency corresponds to the maximum absorption coefficient should be avoided. Furthermore, it is interesting to find that the larger the incident angle is, the smoother the absorption coefficient becomes.

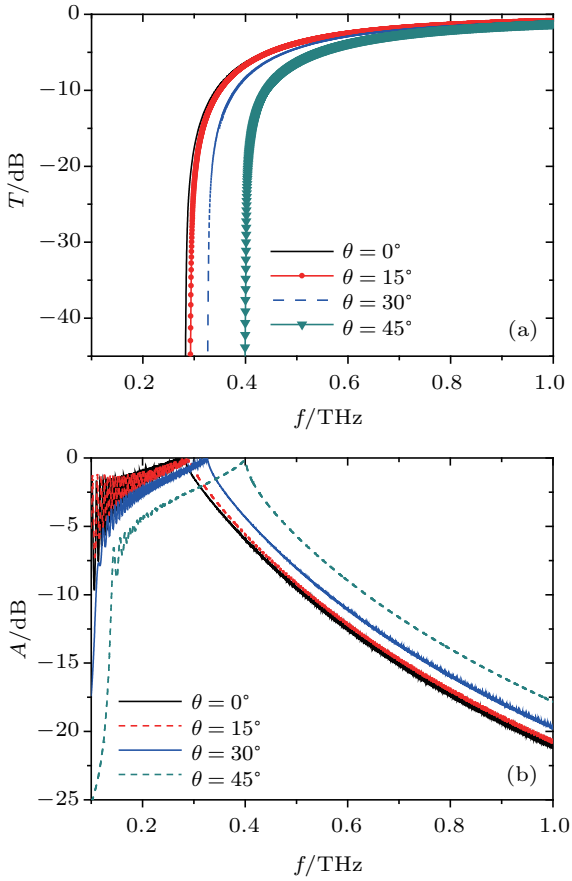


Fig. 4. (a) Transmission and (b) absorption coefficients versus incident angles.

3.3. Influences of thickness

Comparisons of transmission and absorption coefficients for plasma slab of different thickness are displayed in Fig. 5. As shown in Fig. 5, as the thickness of the plasma increases, the transmission coefficient decreases and the absorption coefficient increases. As displayed in Fig. 5(a), in the relatively low frequency range (approximately $f < 0.35$ THz), the plasma thickness has little effect on the transmission coefficient, and the incident EM wave with frequency less than 0.3 THz cannot penetrate the plasma. Similar to the cases shown in Fig. 4(b), there is an absorption peak for each thickness, as shown in Fig. 5(b). Nevertheless, the frequencies corresponding to the absorption peaks are the same for different thickness of plasma slab. It is interesting to find that the increase of the plasma slab thickness broadens the absorption peak.

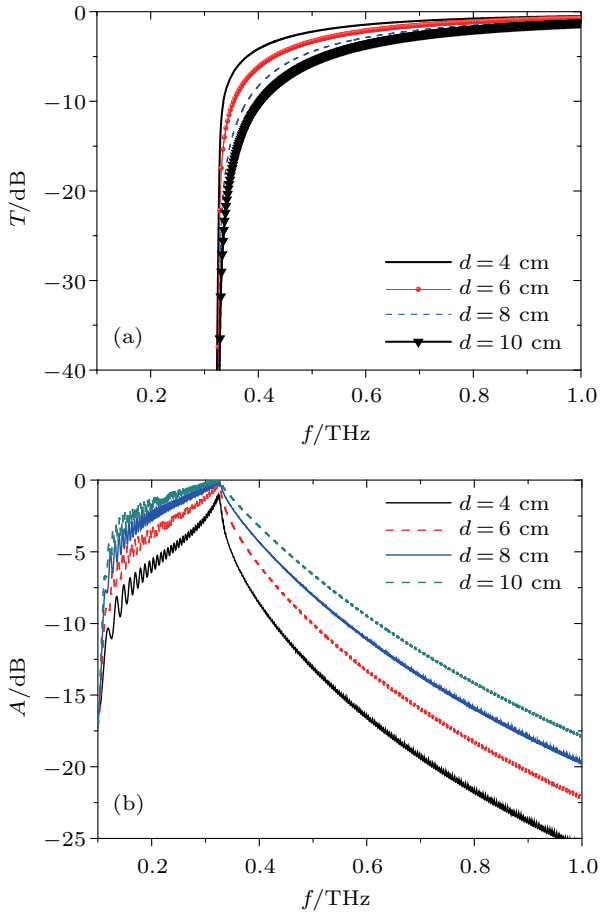


Fig. 5. (a) Transmission and (b) absorption coefficients versus thickness of plasma slab.

3.4. Influences of polarization

Figure 6 illustrates the effects of polarization on the transmission and absorption coefficients. As shown in Fig. 6(a), the polarization of the incident wave has little influence on the transmission coefficient for the cases under study. The transmission coefficient increases as the incident angle decreases or the frequency increases, which is the same as we obtained in Fig. 4(a). For the cases of incident angles 30° and 45°, the transmission coefficients for TM wave and TE wave almost overlapped with each other. Figure 6(b) shows that there is a maximum absorption coefficient for each incident angle and the corresponding frequency is the same for different polarizations. The absorption coefficient increases at first and then decreases as the frequency increases. In addition, as shown in Fig. 6(b), the curve of absorption coefficient for TE wave is much smoother than that for the TM wave case.

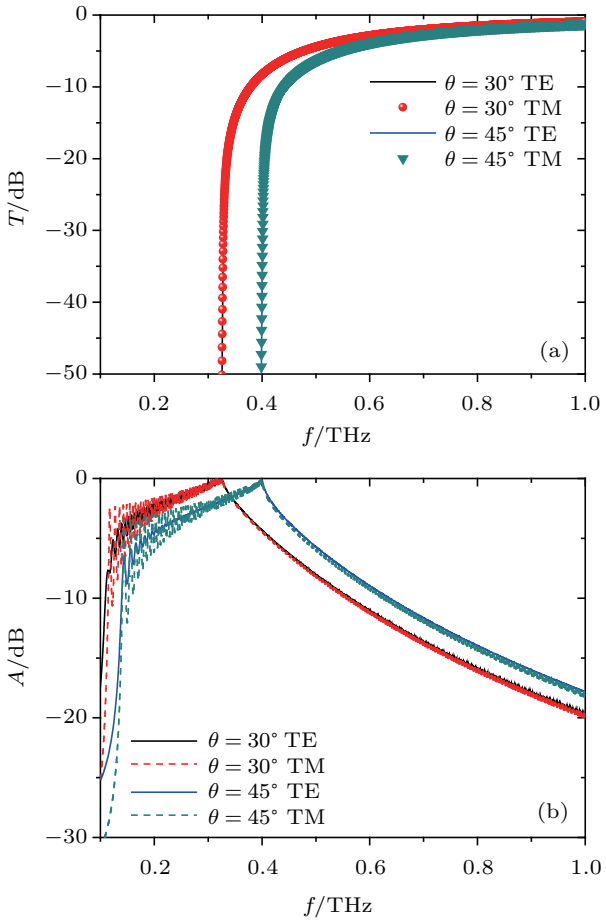


Fig. 6. (a) Transmission and (b) absorption coefficients versus polarization.

4. Conclusion

The variations of power transmission and absorption coefficients for THz wave obliquely incident on a non-uniform plasma slab are analyzed by the SO-FDTD method combined with the phase matching condition. The factors that may affect the propagation characteristics of THz wave through plasma, including the incident angle of the incident wave, the thickness of the plasma, and the polarization of the wave, are studied. The results reveal that the incident angle can affect the propagation properties greatly, while the polarization of the incident wave has little influence on the propagation properties for the cases under study. When the THz wave is employed to the communication in the ionization blackout situation, the

incident angle should be considered, and the frequency corresponding to the maximum absorption should be avoided. This study will be useful to provide a reference for the exploration of potential techniques to overcome ionization blackout problem as well as to provide insights to the interactions between THz wave and plasma.

References

[1] Huber P W, Evans J S and J C J C 1971 *AIAA J.* **9** 1154
[2] Keidar M, Kim M and Boyd I 2008 *J. Spacecr. Rockets* **45** 445
[3] Rybak J P and Churchill R J 1971 *IEEE Trans. Aerosp. Electron. Syst.* **AES-7** 879
[4] Morabito D D 2002 *The Spacecraft Communications Blackout Problem Encountered During Passage or Entry of Planetary Atmospheres*
[5] Zang Q, Bai X, Ma P, Huang J, Ma J, Yu S, Shi H, Sun X, Liu Y and Lu Y 2017 *Opt. Lett.* **42** 687
[6] Hartunian R, Stewart G, Curtiss T, Fergason S, Seibold R and Shome P 2007 *AIAA Atmospheric Flight Mechanics Conference and Exhibit* (Hilton Head, South Carolina: American Institute of Aeronautics and Astronautics) pp. 1-10
[7] Gu L, Tan Z Y and Cao J C 2013 *Physics* **42** 695 (in Chinese)
[8] Wu M, Lang T, Shi G and Han Z 2018 *Opt. Commun.* **410** 520
[9] Panyaev I, Dadoenkova Y, Zolotovskii I and Sannikov D 2018 *Opt. Commun.* **426** 395
[10] Xie Z, He J, Wang X, Feng S and Zhang Y 2015 *Opt. Lett.* **40** 359
[11] Rao Z, Wang X and Lu Y 2011 *Opt. Commun.* **284** 5472
[12] Li J, Pi Y and Yang X 2014 *Wirel. Commun. Mob. Com.* **14** 1252
[13] Li S, Li J, Zhu Z and Cui W 2015 *Int. Conf. Signal Process.* pp. 2398–2402
[14] Yuan C, Zhou Z, Zhang J W and Xiang X 2011 *J. Appl. Phys.* **109** 063305
[15] Yuan C, Zhou Z, Xiang X, Sun H, Wang H, Xing M and Luo Z 2011 *Nucl. Instrum. Methods Phys. Res. B* **269** 23
[16] Yuan C, Zhou Z, Xiang X, Sun H and Pu S 2010 *Phys. Plasmas* **17** 113304
[17] Ling Z, Qing Z, Zhang L S and Jun X X 2012 *Acta Phys. Sin.* **61** 245202 (in Chinese)
[18] Tosun Z, Akbar D and Altan H 2009 *Int. Conf. Infrared Millimeter Terahertz Waves,* pp. 1-2
[19] Guo L J, Guo L X and Li J T 2017 *Phys. Plasmas* **24** 022108
[20] Chen J, Yuan K, Shen L, Deng X, Hong L and Yao M 2016 *Prog. Electromagn. Res.* **157** 21
[21] Wang M, Li H, Dong Y, Li G, Jiang B, Zhao Q and Xu J 2016 *IEEE Trans. Antennas Propag.* **64** 286
[22] Wang M, Yu M, Xu Z, Li G, Jiang B and Xu J 2015 *IEEE Trans. Plasma Sci.* **43** 4182
[23] Zheng L, Zhao Q, Liu S, Xing X and Chen Y 2014 *J. Infrared Millim. Te.* **35** 187
[24] Tian Y, Ai X, Han Y and Liu X 2014 *Phys. Plasmas* **21** 123303
[25] Gao R, Yuan C, Wang Y, Zhou Z, Gong D, Fang Y and Rong X 2013 *J. Appl. Phys.* **114** 123302
[26] Yuan C X, Zhou Z X, Zhang J W, Xiang X L, Yue F and Sun H G 2011 *IEEE Trans. Plasma Sci.* **39** 1577
[27] Chen W, Li J T and Dan L 2017 *Acta Phys. Sin.* **66** 84102 (in Chinese)
[28] Chen W, Deng X J, Feng J, Huang G Y 2014 *Acta Phys. Sin.* **63** 194101 (in Chinese)
[29] Liu S, Zhou T, He X, Zhou Y and Hong W 2006 *Int. Symp. Antennas Propag. EM Theory,* pp. 1-4
[30] Liu S, Zhou T, Liu M and Hong W 2008 *J. Syst. Eng. Electron.* **19** 15
[31] Rahmani Z and Moradi H 2018 *Optik* **155** 81
[32] Yuan K, Chen J, Shen L, Deng X, Yao M and Hong L 2018 *IEEE Trans. Plasma Sci.* **46** 373
[33] Cao Y, Li H, Wang Z and Wu Z 2016 *Int. J. Antenn. Propag.* **2016** 1
[34] Tian Y, Yan W, Gu X, Jin X, Li J and Li B 2017 *AIP Adv.* **7** 125325
[35] Ling Z 2013 *Study of Electromagnetic Wave Propagation in Spacecraft Plasma Sheath* (Ph.D. Thesis) (Chengdu: School of Physical Electronics) (in Chinese)
[36] Sullivan D 2013 *Electromagnetic Simulation Using the FDTD Method* (New York: IEEE Press)